Sex Plant Reprod
DOI 10.1007/s00497-012-0188-1

ORIGINAL ARTICLE

Confocal observations of late-acting self-incompatibility in *Theobroma cacao* L.

Caroline S. Ford · Mike J. Wilkinson

Received: 22 January 2012 / Accepted: 8 May 2012

Abstract Cocoa (*Theobroma cacao*) has an idiosyncratic form of late-acting self-incompatibility that operates through the non-fusion of incompatible gametes. Here, we used high-resolution confocal microscopy to define fine level changes to the embryo sac of the strongly self-incompatible cocoa genotype SCA 24 in the absence of pollination, and following compatible and incompatible pollination. All sperm nuclei had fused with the female nuclei by 48 h following compatible pollinations. However, following incompatible pollinations, we observed divergence in the behaviour of sperm nuclei following release into the embryo sac. Incomplete sperm nucleus migration occurred in approximately half of the embryo sacs, where the sperm nuclei had so far failed to reach the female gamete nuclei. Sperm nuclei reached but did not fuse with the female gamete nuclei in the residual cases. We argue that the cellular mechanisms governing sperm nucleus migration to the egg nucleus and those controlling subsequent nuclear fusion are likely to differ and should be considered independently. Accordingly, we recommend that future efforts to characterise the genetic basis of LSI in cocoa should take care to differentiate between these two events, both of which contribute to failed karyogamy. Implications of these results for continuing efforts to gain better understanding of the genetic control of LSI in cocoa are discussed.

Keywords *Theobroma cacao* · Cocoa · Self-incompatibility · Late-acting SI · Confocal microscopy · Gametic non-fusion

Communicated by Tetsuya Higashiyama.

Electronic supplementary material The online version of this article (doi:10.1007/s00497-012-0188-1) contains supplementary material, which is available to authorized users.

C. S. Ford · M. J. Wilkinson (✉)
School of Agriculture Food and Wine, The University of Adelaide, Waite Campus, PMB 1, Glen Osmond, Adelaide, SA 5064, Australia
e-mail: mike.wilkinson@adelaide.edu.au

Introduction

Cocoa (*Theobroma cacao* L.) is a diploid member of the Malvaceae (Alverson et al. 1998) and is a labour-intensive crop that is cultivated on smallholder farms over most of its range (Sauer 1994). Breeding of the crop has thus far relied heavily on the creation of intraspecific hybrids (Soria 1978; Reyes 1979; Lockwood 1979). Many of the hybrids supplied to farmers were originally generated in large biclonal seed gardens established in cocoa-producing countries between 1960 and 1990. These gardens typically contain substantial stands of trees comprising one pollen parent for every three self-incompatible (SI) seed parents (Efombagn et al. 2009). However, variability in the strength of SI exhibited by the seed parents means that the proportion of hybrids retrieved from these gardens is highly variable (Lanaud et al. 1987). Cocoa operates a late-acting or ovarian form of self-incompatibility, the efficacy of which varies between clonal varieties. The discovery and characterisation of cocoa clones with strong-acting SI may offer benefits for future efforts to generate new elite parental clones capable of producing large numbers of hybrid progenies.

In late-acting self-incompatibility (LSI) systems, self-pollen tubes grow to the ovary without inhibition. Eventual arrest of the incompatible gamete can occur at any point between the integument and the initiation of embryogenesis

Published online: 27 May 2012

and may be followed by the rejection of an entire ovary via floral abscission. Such late-acting mechanisms operate in a variety of plant groups and are believed to have evolved many times throughout the evolution of the angiosperms (Allen and Hiscock 2008; Seavey and Bawa 1986).

The timing and site of male gamete arrest can occur pre-zygotically: for example, in the placenta or micropyle (Myrtaceae, Beardsell et al. 1993), within the embryo sac via failure of fusion (Fagaceae, McKay 1942; Malvaceae, Cope 1940) or female gamete degradation (Amarylliadaceae, Sage et al. 1999); or post-zygotically: for example via the failure of zygotic division (Bombacaceae and Bignoniaceae, Gibbs and Bianchi 1993; Ericaceae, Williams et al. 1984; Asclepiadaceae, Sage and Williams 1991) or endosperm development (Winteraceae, Sage and Sampson 2003).

The genetic basis of many of these reactions is not known. Given the ovarian nature of the rejection reaction, it would seem more likely that they are under gametophytic control and are often hypothesised as such (Sage et al. 1994). If these systems were sporophytically controlled, long-distance signalling events and elaborate cascades would need to be in operation (Sage et al. 1999). In species where sperm cells are delivered to the embryo sac but fail to fuse, it has been suggested that elements of the recognition/rejection response may operate at gamete plasma membranes (Knox et al. 1986; Sage et al. 1994). Alternatively, recognition reactions may be operating in the placenta or the integument, but the consequences of the resultant cascade are not manifest until after the sperm cells have been released (Sage et al. 1994).

In addition to the well-characterised examples, many species have been recorded as possessing LSI based solely on observations of uninhibited pollen tube growth to the ovule (e.g. Gibbs and Bianchi 1999; Gribel and Gibbs 2002; Gribel et al. 1999; Kawagoe and Suzuki 2005; LaDoux and Friar 2006; Oliveira and Gibbs 2000; Sage et al. 1999; Taroda and Gibbs 1982; Vaughton et al. 2010). To gain a greater understanding of the operation of varied LSI systems and their genetic control, further investigation into the timing and site of the rejection reaction within the ovule is required.

Self-incompatibility in *Theobroma cacao*

Pound (1932) first noted that some cocoa genotypes are self-incompatible. Anatomical works by Cope (1939, 1940) revealed that gametic fusion often failed to complete in ovules subjected to incompatible pollination, indicating that SI operated via a post-fertilisation process in which the failure of gametic fusion in a proportion of ovules in an ovary ultimately lead to floral abscission (Cope 1940). Knight and Rogers (1955) later observed that the incompatibility reaction occurred after the release of male gametes into the embryo sac, which prevented syngamy and was thus pre-zygotic. Further work by Cope (1958) provided the first evidence from *T. cacao* of a species using 'non-fusion of gametes' as its rejection method in the operation of LSI.

Later works have revealed that this system is not confined to *T. cacao* and has been reported in closely related species within the old family of the Sterculiaceae (now Malvaceae, Alverson et al. 1998). Observations of post-pollination events in *Sterculia chicha* (Taroda and Gibbs 1982), *Dombeya acutangula* (Gigord et al. 1998), *Theobroma grandiflorum* (Ramos et al. 2005), *Theobroma speciosum* (de Sousa and Venturieri 2010) and *Cola nitida* (Jacob 1973) show that pollen tubes grow uninhibited to the ovary but fail to set seed.

There has been considerable debate over the mode of genetic control of SI in cocoa. Knight and Rogers (1953, 1955) used the results from a series of controlled crosses to postulate that the system was under sporophytic control, with the diploid constitutions of both parents being involved in determining the compatibility of a cross. They argued that a single S locus exhibits both dominance and independence relationships. Bouharmont (1960) subsequently challenged this view by reasoning that cytological evidence and the existence of hemi-compatibility in some crosses suggests that SI is under gametophytic control. More comprehensive studies by Cope (1958, 1962) repeated the crosses made by Knight and Rogers and extended the scope of the work to encompass around 100 clones. This revealed three types of segregation ratios among the ovules of pollinated flowers, viz: 1:3, 1:1 and 1:0 ('non-fused': 'fused' ovules), of which the first was by far the most common. The author noted that this clearly points towards the haploid genotype determining the capacity to effect gametic fusion (i.e. gametophytic control). However, he went on to postulate that this property could give the appearance of sporophytic control if one assumed that 'non-fusion' occurred when the alleles carried by egg and sperm were identical. In such instances, all gametes would fuse only when both parents contained different alleles. This explanation was insufficient in itself to accommodate for the apparent dominance of some alleles as inferred from crosses between related genotypes. For example, when genotypes $S_{2.3}$ and $S_{2.5}$ from the Knight and Rogers (1955) study were crossed, 25 % of ovules did not fuse but when $S_{2.5}$ and $S_{1.2}$ were crossed, gametes fused in all ovules. Knight and Rogers (1955) explained this by proposing that S_2 is dominant to S_5. However, this reasoning requires that the seemingly implausible condition that the S locus has a two-step action: one before meiosis to establish dominance and one after meiosis to provide the reaction between gametes. Detailed analysis of a series of F_2 crosses led

Cope (1962) to further reason that there must be at least two accessory loci (A and B) and that these genes are sporophytically expressed in the gametes. It was thus argued that three independent genes exist (A, B and S), along with two levels of control (sporophytic and gametophytic) (Cope 1962). Even at the time, the author recognised that this rather ornate genetic explanation is difficult to reconcile with known biological processes. It has nevertheless persisted to the present day as the preferred genetic explanation of this strange biological phenomenon.

One possible constraint with these early studies could be attributed to the limited resolution of the cytological observations. In part, this may have been because all observations were based on 5–15 μm sections variously stained (crystal violet, iron haematoxylin, gentian violet, safranin) and viewed using a light microscope. It is possible that impaired sperm nucleus behaviour was not visible or could not be deciphered from such sample preparations, and so it could not be determined whether the lack of fertilisation was caused by failure of nuclear fusion or by incomplete or delayed sperm nucleus migration. Disentanglement of these events may provide the opportunity to simplify the elaborate genetic explanation of LSI in cocoa. In the present study, we therefore use the enhanced resolution afforded by confocal microscopy to provide a more detailed description of the events following male gamete release from the pollen tube after compatible and incompatible pollinations of a SI cocoa clone. We also examine the cytological changes that occur in unpollinated ovules over the same time period.

Materials and methods

This work was conducted using cocoa accessions held in the International Cocoa Quarantine Centre at The University of Reading, UK. Preliminary work selected 25 genotypes from the collection previously reported to be self-incompatible, and two that were self-compatible (Turnbull and Hadley 2011) (Supplementary Data Table S1). The self-compatibility reaction of each of these trees was confirmed by hand-pollination. Staminodes were removed from the pollinated flower to improve access to the stigma, and self-pollinations were affected using 2–3 stamens from a separate flower of the same tree; both flowers were within 6 h of anther dehiscence. Twenty self-pollinations were performed on each genotype. Pollinations were deemed to be 'compatible' if the flower had not abscised after 5 days and the peduncle had begun to thicken; flowers with an incompatible reaction had normally abscised within 4 days. Based on these results (Supplementary Data Table S1) and on the abundance of flowers for further work, the 100 % self-incompatible genotype SCA 24 was selected for more detailed cytological examination.

Flowers of SCA 24 were subjected to one of three pollination treatments: unpollinated (no treatment), compatible pollination and incompatible (self) pollination. Compatible pollinations were performed by hand as described above using stamens from the cross-compatible clone PA88 [PER]. Incompatible (self) pollinations were performed using the same method with stamens from separate flowers from SCA 24. Treated flowers were retained on the tree for 8, 24, 36, 48, 72 or 96 h (96 h was possible only after compatible pollinations). After this, they were removed and fixed in 3:1 (v/v) ethanol: glacial acetic acid for at least 24 h. Fixed flowers were stored in 70 % ethanol at 4 °C until required.

Intact ovaries were isolated from fixed flowers, subjected to Feulgen staining and embedded in LR white resin (soft) using the following protocol adapted from Braselton et al. (1996). In brief, fixed ovaries were first rinsed three times in reverse osmosis (RO) water (15 min each rinse), hydrolysed in 5 M HCl (1 h), followed by a further three rinses in RO water (5 min each). Samples were stained in Periodic Schiff's Reagent or 5 μg ml^{-1} aqueous propidium iodide for 2–3 h at room temperature, or else in 2 μg ml^{-1} DAPI in McIlvaine's buffer (0.1 M citric acid, 0.2 M Na_2HPO_4, pH 7) at 4 °C overnight. Following staining, samples were again rinsed three times in cold RO water (10 min each) and passed through an ethanol dehydration series comprising 70 % ethanol (10 min) followed by 3-5 changes of 100 % ethanol (10 min each). Ovaries were then incubated in 1:1 (v/v) ethanol: LR white (1 h), transferred to 100 % LR white (1 h), with a final incubation overnight in fresh 100 % LR white. Ovules were dissected from the ovary onto a microscope slide and mounted in LR white. Slides were incubated at 60 °C for 24 h to polymerise the LR white resin.

Mounted ovules stained with Periodic Schiff's Reagent and propidium iodide were observed at 400× magnification using a Leica TCS-NT confocal laser-scanning microscope with an argon laser at a wavelength of 568 nm. Images were analysed using the Leica Confocal Software package version 2.5, build 1104 and are presented with the false colour mask 'glow'. Ovules stained with DAPI were observed at 400× magnification using a Leica DMIRE2 confocal laser-scanning microscope with an argon laser wavelength of 458 nm and analysed using Leica Confocal Software package version 2.4, build 1227. The Leica software was used to measure relative proximity of sperm nuclei to nuclei of female gametes in ovules fixed 24, 36 and 48 h after compatible and incompatible pollinations. The distance between sperm nuclei and both the egg and nearest polar nucleus was measured in silico from nuclear membrane to nuclear membrane. These measurements

were only possible in a minority of observed ovules where both the egg and polar nucleus and any remnant sperm nuclei were present and clearly defined in the same optical section. Nuclear volume was estimated from the formula: $4/3\pi r^3$ using mean radii (r) measurements.

The images presented are stained with Periodic Schiff's Reagent (unless otherwise stated, Supplementary Data) and prepared for publication using Photoshop version 7.0.

Results

The self-compatibility screen of 27 clones revealed that for the majority (18/25) of clones reported to be self-incompatible, floral abscission occurred after all 20 self-pollinations. The remaining seven 'self-incompatible' genotypes retained between one and two of the 20 self-pollinated flowers. Genotypes previously described as 'self-compatible' retained only marginally more flowers, with just four out of 20 flowers remaining on the tree following self-pollination (Supplementary Data Table S1). Thus, this initial screen confirmed the notoriously blurred demarcation between self-compatible and self-incompatible genotypes in cocoa. In order to avoid such ambiguity in the cytological investigations, the 100 % self-incompatible and most floriferous tree SCA 24 was used in all subsequent confocal examinations.

Approximately 200 ovules were observed and images of 88 ovules were captured from unpollinated flowers of SCA 24 sampled 24, 36, 48 and 72 h after flower opening. At 24 h, these samples contained an oval embryo sac measuring 39.27 ± 10.73 μm ($2 \times$ standard deviation) diameter in transverse section and 56.11 ± 8.49 μm longitudinally (Fig. 1a). The synergid cells extended 20.92 ± 3.82 μm into the embryo sac and were commonly vacuolated at the antipodal end (Fig. 1b, c). The nuclei of the synergid cells were clearly visible within the central section of the cell (Fig. 1b, c). The egg cell typically sat alongside or underneath the synergid cells, depending on the orientation of the ovule, with the nucleus always positioned proximal to the synergid cells (Fig. 1b, d). The polar nuclei were positioned near the chalazal end of the synergid cells within the central area of the embryo sac (Fig. 1b, c). Starch grains were usually clearly visible and tended to cluster around the polar nuclei, sometimes surrounding them completely (Fig. 1b, c). As the unpollinated flower aged, the vacuoles of the synergid cells became enlarged and extended further into the embryo sac (Fig. 2a at 36 h). By 48 h after flower opening, the synergid cells had grown to 26.97 ± 4.64 μm in length (Fig. 2d). The egg cell had become distended and irregular in shape, and the nucleus had moved above the level of the synergid cells as the cell increased in size (Fig. 2b, c). The polar nuclei showed no visible symptoms of ageing and apparently remain unchanged throughout this period (Fig. 2a, c). By 72 h after flower opening, ovules were difficult to obtain as flowers had usually abscised prior to this point. In the few cases where it was possible to secure ovules from flowers, the DNA appeared to have significantly degraded in all cells to such an extent that the egg apparatus was no longer clearly defined.

We observed approximately 300 ovules and collected images of 115 ovules from compatibly pollinated flowers sampled 8, 24, 36, 48, 72 and 96 h after pollination. Eight hours after a compatible pollination, the pollen tubes had not yet reached the embryo sac or the ovule (Fig. 3a). At this point, both synergid cells remained intact and pollen tubes had not reached the integumentary tissues of the ovule. Twenty-four hours after pollination, however, there was clear evidence of synergid degradation, pollen tube penetration and gamete release (Fig. 3b–d). In most samples collected at this stage (43/50), the pollen tube had penetrated the integumentary tissues and progressed into the degenerated synergid cell (Fig. 3b). In all of these ovules (43/43), the two sperm cells and accompanying vegetative nucleus had been released from the pollen tube and in some cases (13/43), the sperm cells had emerged through the end of the degenerated synergid: one gamete in proximity to the egg cell and the other advancing towards the central cell (e.g. Fig. 3b–d). In a small minority of cases (3/43), double fusion had already occurred. In almost all cases (40/43), the central cell contained two distinct polar nuclei, with each nucleus containing a distinct nucleolus. The vegetative nucleus remained within the body of the degenerated synergid cell in all cases, along with the degrading synergid nucleus (Fig. 3c, d). Double fertilisation had occurred in most ovules by 36 h after pollination, fusion having occurred between one sperm nucleus and the egg nucleus, the second sperm nucleus and one polar nucleus. At this time, the clearest signs of pollen tube arrival were the disrupted degenerated synergid cell and the brightly stained vegetative nucleus within it (Fig. 4b). The newly formed zygote nucleus in these samples was marginally larger than the egg nucleus in the unpollinated embryo sacs (182.53 ± 44.18 μm^3 vs. 148.63 ± 60.18 μm^3, respectively). Furthermore, zygotic nuclei generally migrated slightly lower in the egg cell to occupy a position below the chalazal end of the synergid cells and towards the micropylar end of the embryo sac (Fig. 4a). The central cell of these ovules invariably contained two distinct nuclei: presumably one diploid primary endosperm nucleus and one haploid polar nucleus. In some cases (13/28 of the images captured at this stage), the central cell was positioned towards or against the wall of the embryo sac (Fig. 4a). There was very little further change among samples collected 48 h after pollination. The newly formed

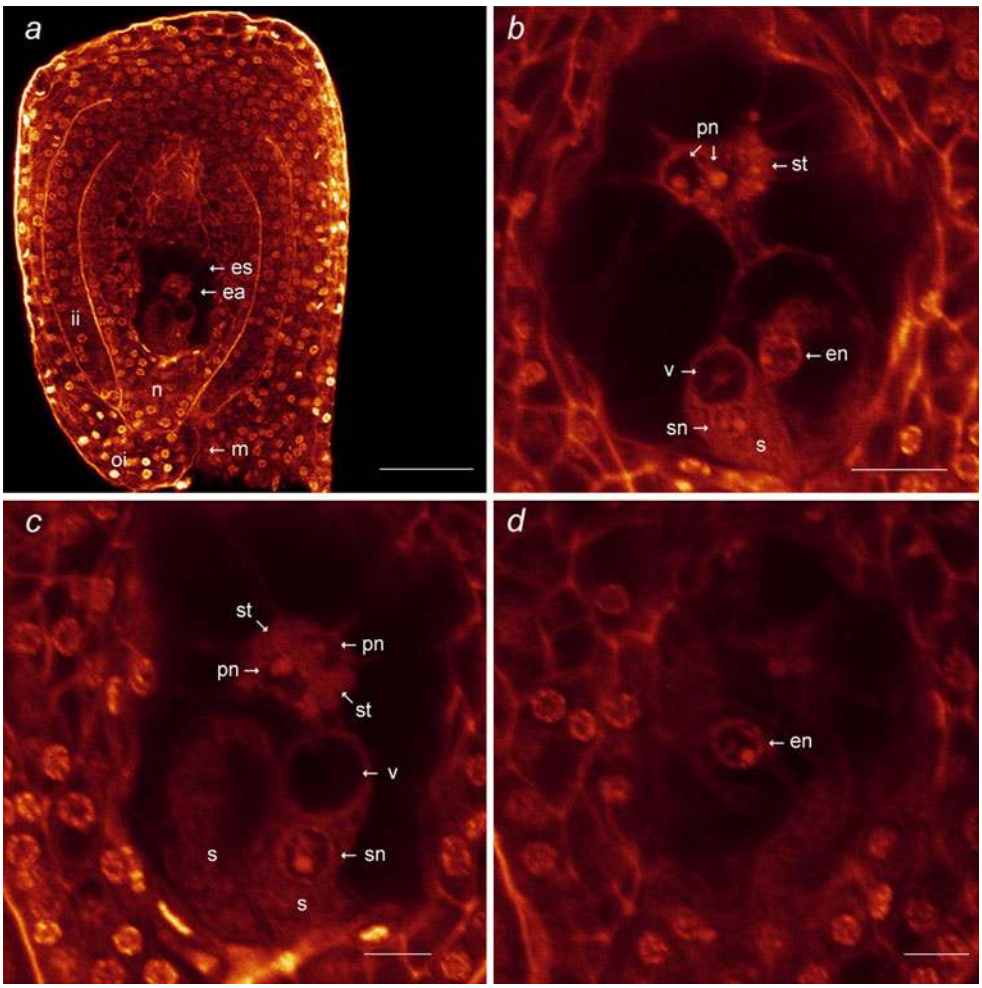

Fig. 1 Unpollinated ovules at 24 h after flower opening. The arrangement of the egg apparatus within the embryo sac. **a** Optical section through an entire ovule showing the micropyle (*m*), outer integument (*oi*), inner integuments (*ii*), nucellus (*n*) and the embryo sac (*es*) containing the egg apparatus (*ea*). *Bar* = 40 µm. **b** Synergid cell (*s*) with nucleus (*sn*) and vacuole (*v*); egg cell positioned alongside the synergid cell with the nucleus (*en*) in close proximity to the end of the synergid; polar nuclei (*pn*) positioned towards the centre of the embryo sac, with surrounding starch grains (st). *Bar* = 16 µm. **c** Synergid cells (*s*); synergid nucleus (*sn*) visible in the right-hand synergid along with a large vacuole (*v*); two polar nuclei (*pn*) positioned near the end of the synergid cells with starch grains (*st*) present. *Bar* = 8 µm. **d** Egg cell from the same ovule as **c** with nucleus (*en*) clearly visible (the egg cell is positioned beneath the synergid cells shown in **c**). *Bar* = 8 µm

zygote nucleus and nuclei of the central cell remained in similar positions, with the zygote nucleus (now 8.39 ± 1.81 µm × 8.62 ± 1.49 µm, with a volume of 340.35 μm^3) sinking low in the embryo sac and the central cell nuclei frequently observed against the embryo sac wall (Fig. 4c, d). The central cell was still usually comprised of two visible nuclei, but these now contained nucleoli that differed considerably in size (Fig. 4c, d), the primary nucleolus being approximately 2 µm in diameter (Fig. 4c) and the second roughly half the size (Fig. 4d). Occasionally (10/30 images), ovules contained three nucleoli in the central cell. By 72 h after pollination, the central cell still mostly contained two distinct nuclei with asymmetric nucleoli (Supplementary Data, Fig. S1a, b). The size difference again usually approximated to one nucleolus being half the size of the other, although nucleoli of equal size were also observed occasionally (Supplementary Data Fig. S1c). At 96 h after pollination, the synergid cells had almost completely degraded and the nucleus of the zygote sat alone at the micropylar end of the embryo sac (Supplementary Data, Fig. S2a–c). Here, the fertilised nuclei of the central cell typically rested against the wall of the embryo sac. The nuclei still contained two visible nucleoli at this point, but membranes separating the two nuclei were less distinct (Supplementary Data, Fig. S2a, b).

There were also larger scale changes to the ovule. For example, ovule wall growth was often apparent by 48 h after compatible pollination as the ovule walls contained more cells, particularly at the micropylar end (Fig. 5c, d), than those of unpollinated ovules collected at the same

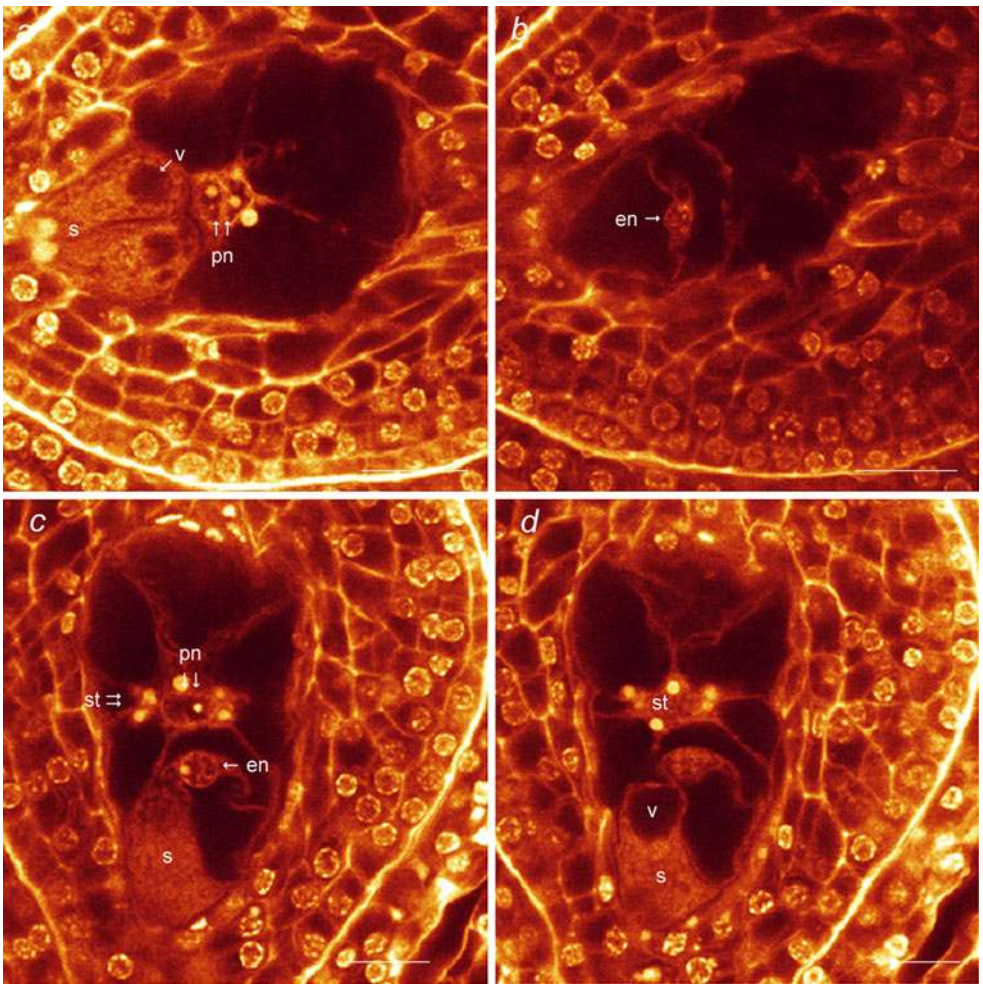

Fig. 2 Unpollinated ovules at 36 and 48 h after flower opening. **a**, **b** Optical sections taken from the same ovule 36 h after flower opening; **c, d** from the same ovule 48 h after flower opening. **a** Synergid cells (*s*) with vacuoles (*v*) and polar nuclei (*pn*). **b** Egg cell and nucleus (*en*). **c** Synergid cell (*s*) and egg nucleus (*en*) are in close proximity; polar nuclei (*pn*) with surrounding starch grains (*st*). **d** Vacuolation (*v*) of the synergid cell (*s*). *Bar* **a–d** = 16 µm

stage (Fig. 5a, b). The tissues of the inner integuments also extended towards the micropylar end, thereby reducing the size of the micropylar opening. The outer integuments extended beyond the micropylar opening, concealing it completely (Fig. 5c, d). Overall, the ovules appeared more rounded in shape (e.g. 195 µm across the transverse diameter, and 215 µm longitudinally, Fig. 5c, d) compared to the more obovate unpollinated ovules (e.g. 170 by 205 µm) (Fig. 5a, b).

We next captured 107 images from approximately 300 observed ovules 24, 36, 48 and 72 h after incompatible self-pollination. As in the compatibly pollinated ovules, pollen tubes had released the male gametes by 24 h. Accordingly, the degenerated synergid showed clear signs of disruption and pollen tube entry (Fig. 6a, b), and the degrading vegetative nucleus from the pollen tube was usually clearly visible within the body of the synergid cell (Fig. 6b). Most commonly, one sperm nucleus was in close proximity to the egg nucleus (Fig. 6a), the second sperm nucleus apparently close to the polar nuclei (Fig. 6b). There was very little change in the position of these proximal male gamete nuclei after 36 h (Fig. 6c, d). Likewise, male and female gamete nuclei remained nearby or adjacent but unfused after 48 h and 72 h (Supplementary Data, Fig. S3a-c), although the egg apparatus was less distinct in the latter, as these ovules had begun to senesce. In some ovules, the central cell had become disorganised by 72 h, with starch grains becoming smaller, making differentiating between starch grains, the nucleoli of the polar nuclei and the sperm nucleus more difficult (Supplementary Data, Fig. S3d). In a small minority (9/107) of incompatible ovules isolated between 24 and 72 h, there was visible evidence of pollen tube entry but without the presence of unfused sperm nuclei within the embryo sac. Gametic fusion and subsequent nuclear fusion were assumed to have occurred in these ovules.

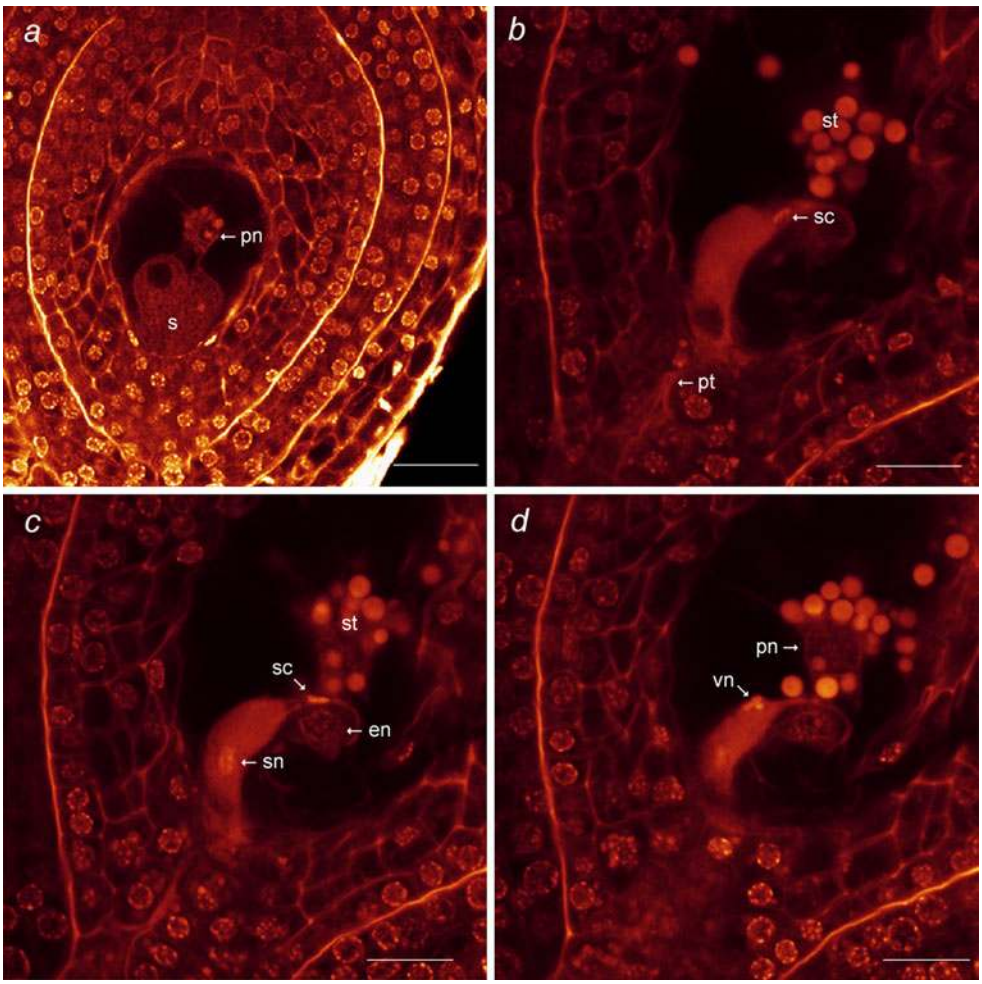

Fig. 3 Compatible ovules at 8 and 24 h after pollination. **a** 8 h After pollination, no visible signs of pollen tube entry to the embryo sac or ovule, synergid cells (*s*) remain intact, polar nuclei (*pn*) visible with some starch grains present. *Bar* = 20 μm. **b–d** Optical sections through the same ovule 24 h after pollination showing the arrival of the pollen tube and release of the male gametes. *Bar* = 12 μm. **b** The pollen tube (*pt*) has grown through the micropyle and integumentary tissues into the synergid cell; a sperm cell (*sc*) can be seen emerging from the end of the synergid; numerous starch grains (*st*) are present. **c** An additional sperm cell (*sc*) has emerged from the synergid and is progressing towards the egg nucleus (*en*); degrading synergid nucleus (*sn*) visible within the synergid; starch grains (*st*) numerous. **d** Showing the position of one of the two polar nuclei (*pn*) within the starch grains; vegetative nucleus (*vn*) visible within the synergid

Post-release movement of sperm nuclei

Overall, among the selected images in which gamete proximity could be measured, arrival of the sperm nucleus at the egg nucleus appeared marginally more rapid than at the polar nuclei following both compatible and incompatible pollinations. Sperm nuclei were on average (across all pollination treatments) between 2.86 and 8.02 μm further from the polar nucleus than they were from the egg nucleus (Table 1). In a qualitative sense, there were six instances where sperm and egg nuclei were in direct membrane contact, but sperm and polar nuclei were still separate (mean = 2.04 μm). Furthermore, there was one ovule where sperm-egg nuclear fusion had occurred, but sperm and polar nuclei remained separated by 1.32 μm (Table 1). There were no ovules where the reverse was true (Table 1).

Following compatible pollinations (where distance could be measured), the mean separation between sperm nuclei and either the egg nucleus or the polar nuclei progressively reduced between 24 and 36 h (Table 1). Taken collectively, the proportion of sperm-egg and sperm-polar nuclear fusions increased from 0/20 ovules at 24 h to 13/20 at 36 h and 20/20 at 48 h (Table 1). Thus, while there was considerable ovule-to-ovule variation, there was a clear progression towards syngamy over this period.

Intracellular movement of the two sperm nuclei was initially similar following incompatible pollination, with both sperm nuclei reaching the embryo sac by 24 h and no significant difference in separation between the sperm and

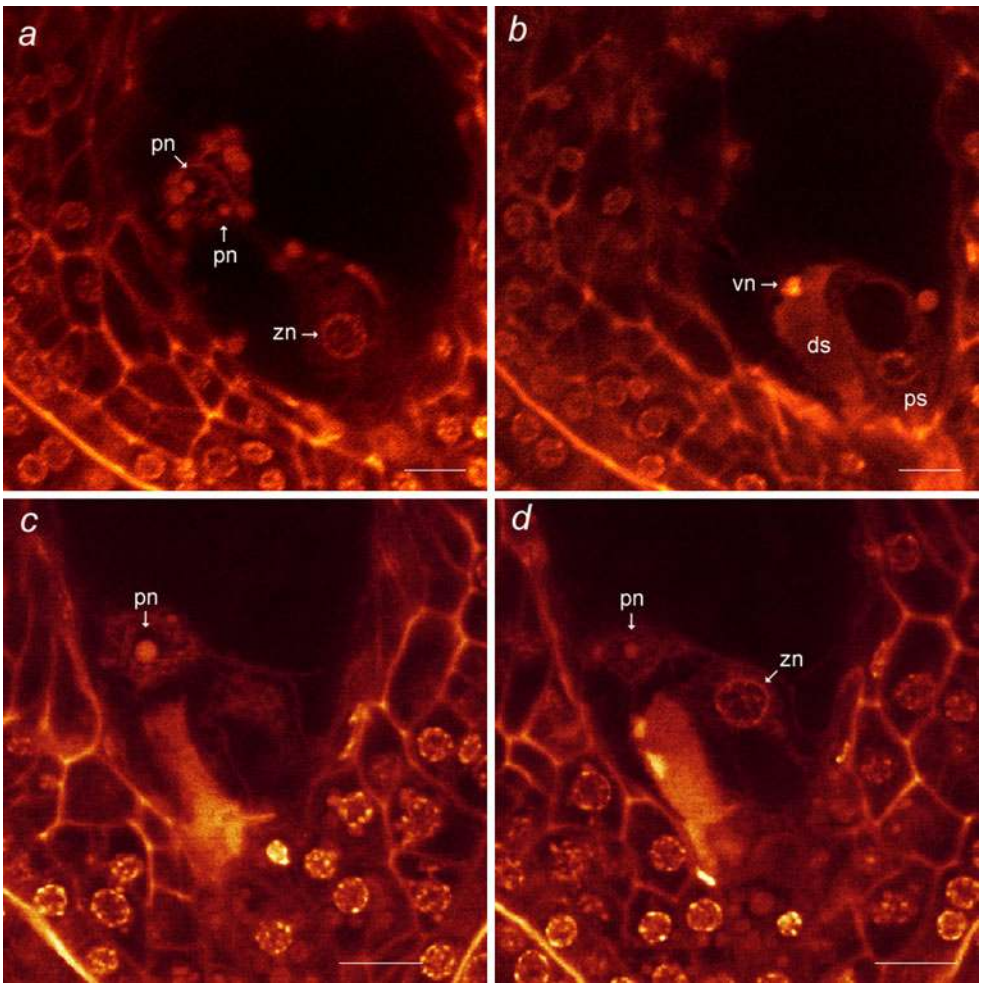

Fig. 4 Compatible ovules at 36 and 48 h after pollination. **a**, **b** Optical sections through the same ovule at 36 h after pollination. **c, d** Optical sections through the same ovule at 48 h after pollination. **a** The zygote nucleus (*zn*) remains in a similar position within the embryo sac post-syngamy and polar nuclei/endosperm nuclei (*pn*) start to move towards the embryo sac wall. **b** The vegetative nucleus (*vn*) present within the degenerated synergid (*ds*) is now the only visible x-body, the nucleus and vacuole of the persistent synergid (*ps*) are still visible. **c** Polar nucleus/endosperm nucleus (*pn*) containing a single, large nucleolus. **d** Zygote nucleus (*zn*); polar nucleus/endosperm nucleus (*pn*) containing a single nucleolus, smaller in size than that in **c**. *Bar* **a**–**d** = 8 μm

their target female nuclei (Table 1). Differences between the two treatments (compatible and incompatible pollination) first became apparent by 36 h after pollination. At this point, 15/20 sperm nuclei had yet to reach either female gamete nucleus after incompatible pollinations compared with 7/20 following compatible pollinations ($\chi^2 = 6.47$ with 1 degree of freedom, $p = 0.011$**; Yates' correction for continuity $\chi^2 = 4.95$ with 1 degree of freedom, $p = 0.026$*). However, the residual distance between the undelivered sperm nuclei and their target nuclei was comparable between the two treatments ($p = 0.552$, $p = 0.649$, Table 1). Double fertilisation including karyogamy occurred in 60 % of compatible ovules by this time, but did not occur in any of the incompatible ovules (Table 1).

There was marked divergence between treatments by 48 h. Among the images where separation measurements were possible (Table 1), approximately half (15/32) of sperm nuclei in the incompatible ovules were adjacent to but not fused with their target female gamete nucleus. The remaining sperm nuclei (17/32) invariably lay within 20 μm of the female gamete nuclei, with a mean separation of 6.03 ± 5.10 μm. This is consistent with a 1:1 segregation for gamete nucleus delivery/non-delivery (Table 1, $\chi^2 = 0.13$, 1 degree of freedom, $p = 0.72$). Double fertilisation occurred in 100 % of compatible ovules by this time, but there was no nuclear fusion among incompatible ovules where measurements were possible (Table 1).

Discussion

It has been 50 years since the last detailed cytological study of self-incompatibility in cocoa (Cope 1962). One objective of the present study was to use the higher

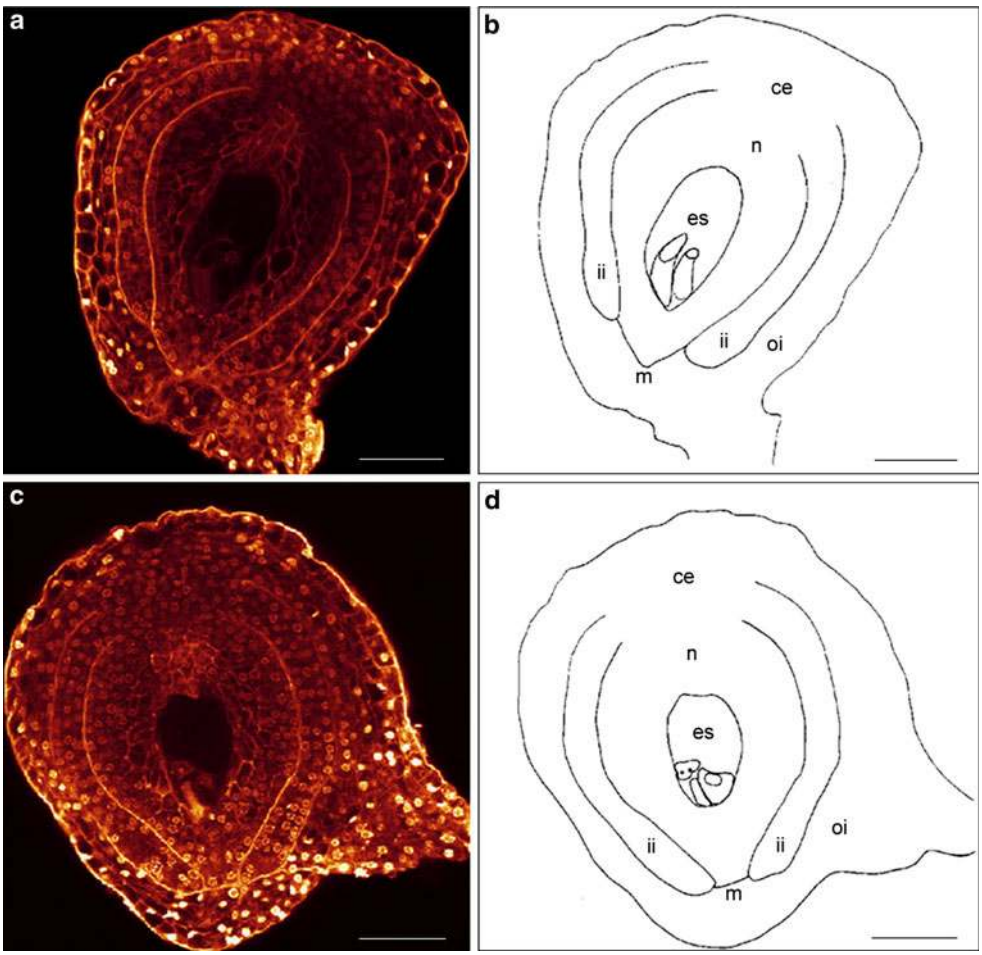

Fig. 5 Whole ovules at 48 h after flower opening. **a**, **b** Confocal image with a line drawing representation of an unpollinated ovule 48 h after flower opening; embryo sac (*es*), nucellus (*n*), inner integuments (*ii*), outer integuments (*oi*), micropyle (*m*), chalazal end (*ce*). **c**, **d** Confocal image with a line drawing representation of a compatibly pollinated ovule at 48 h after pollination; embryo sac (*es*), nucellus (*n*), inner integuments (*ii*), outer integuments (*oi*), micropyle (*m*), chalazal end (*ce*). Evidence of the growth of the ovule wall seen most markedly at the micropylar end as the inner integuments have extended to reduce the size of micropylar opening and the outer integuments have grown round to cover and conceal the micropyle (*m*). Growth is also apparent at the external surface of the ovule wall. *Bar* **a**–**d** = 40 μm

resolution images offered by confocal microscopy to re-examine the cytological processes associated with LSI in cocoa. Overall, we found excellent congruence between the observations made here and those reported previously but were also able to add to the knowledge base of the system in several ways. The first of these arose from the use of unpollinated control material. Floral abscission marks the final part of the incompatibility reaction in cocoa but also occurs in the absence of pollination. It is therefore important to distinguish between changes that occur to the embryo sac in the absence of pollination from those that arise from LSI following incompatible pollinations. Several authors have adopted this premise when studying the effect of hormonal changes on the abscission layer of pedicels associated with floral drop following incompatible pollinations (Aneja et al. 1999; Baker et al. 1997; Hasenstein and Zavada 2001). In the present study, we examined 200 intact unpollinated ovules 24, 36 and 48 h after flower opening. At 24 h, the structure of the embryo sac was much the same as that described by Cheesman (1927), with two large synergid cells, both of which have a tendency to be vacuolated at the antipodal end, one large egg cell and two smaller polar nuclei, surrounded by numerous starch grains. There were subtle changes to the synergid cells and the egg cell of unpollinated ovules associated with age but not to the polar nuclei. Most notable of these occurred by 48 h and included a marked increase in the size of the synergid cells mediated through the rapid expansion of the vacuoles and a more subtle expansion of the egg cell. However, given that synergid penetration had occurred by 24 h in both compatible and incompatible pollinations, such perturbations to the synergid cells have little relevance to events linked with gamete fusion or to any LSI-associated response. The slight expansion of the egg cell seems similarly unlikely to impact on any LSI-induced change, although it may marginally increase the intracellular distance required for gametic nuclear fusion. Almost all flowers had dropped by 72 h and those that remained had undergone extensive nuclear degradation. All fertilisations had occurred by this time among the compatible crosses, and so this development has only marginal relevance to any LSI-induced change found in the 'incompatible' ovules. Thus, images of the unpollinated ovules of cocoa collectively suggest a largely stable and undisturbed

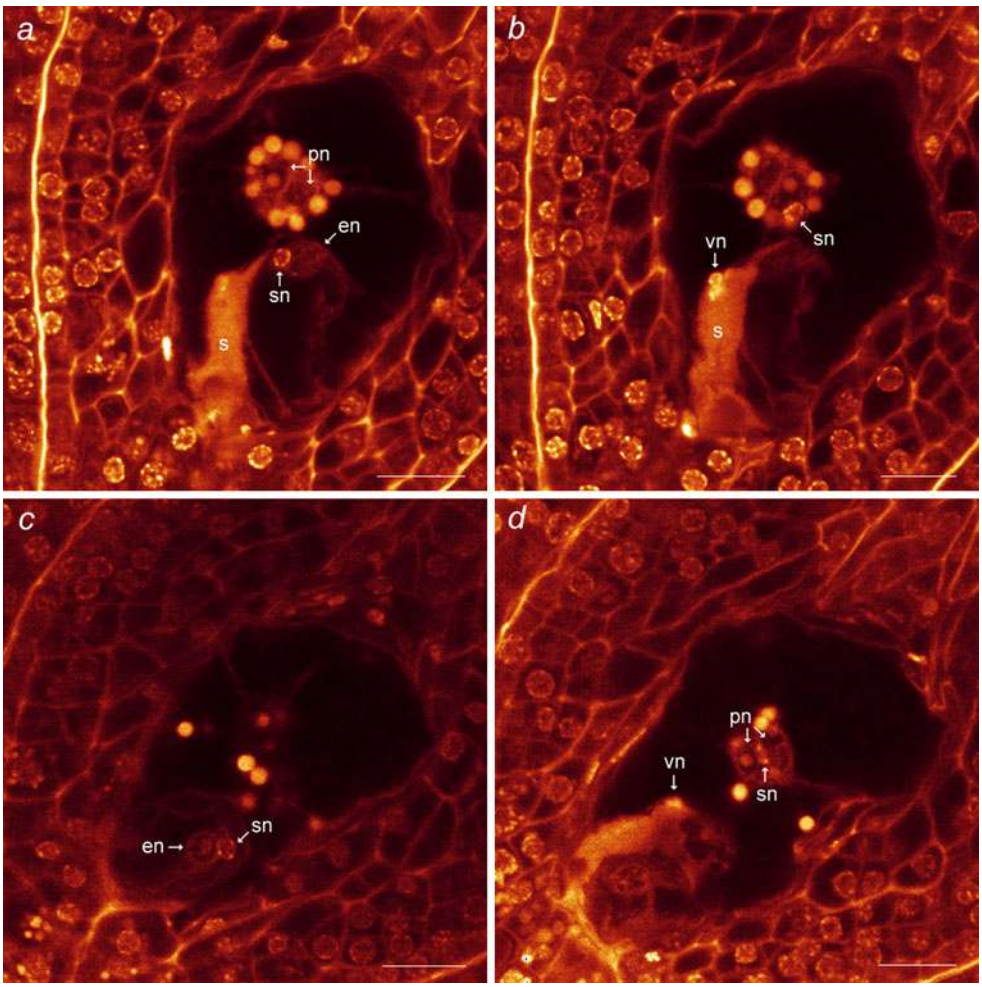

Fig. 6 Incompatible ovules at 24 and 36 h after pollination. **a, b** Optical sections from the same ovule at 24 h after pollination; **c**, **d** Sections through the same ovule 36 h after pollination. **a** Sperm nucleus (*sn*) has been released from the synergid cell (*s*) and is positioned next to the egg nucleus (*en*); polar nuclei (*pn*) are surrounded by starch grains. **b** Sperm nucleus (*sn*) positioned next to one of the polar nuclei; vegetative nucleus (*vn*) can be seen within the degenerated synergid (*s*). **c** Sperm nucleus (*sn*) has penetrated the wall of the egg cell and is next to the egg nucleus (*en*). **d** Sperm nucleus (*sn*) positioned between the two polar nuclei (*pn*); vegetative nucleus (*vn*) visible within the degenerated synergid cell. *Bar* **a**–**d** = 16 μm

arrangement of the embryo sac between the expected time of sperm release and syngamy.

Failure of gametic nuclear fusion provides the first visible signs of the late-acting system of SI exhibited by cocoa (Cope 1940), although it remains unclear whether the failure is attributable to late/incomplete sperm nucleus delivery or an inability to effect nuclear fusion. For this reason, attention in this study focussed on assembling comparable images to allow the progress of sperm nuclei to be 'mapped' within the embryo sac following compatible and incompatible pollinations. The 115 images collected from compatible ovules indicate that pollen tube growth and sperm delivery to the embryo sac were slower than described by Cheesman (1927, 1932) and far more congruent with the later observations of Bouharmont (1960). Moreover, no pollen penetration of the ovule had occurred by 8 h, but it was almost ubiquitous by 24 h after pollination, with double fertilisation taking place soon afterwards. Taken together, the images provide evidence that the sperm released to the egg is the first to fuse (Fig. 3c). We did not see transit of the sperm through the wall of the egg cell in any image, implying that entry into the egg cell is relatively rapid; a supposition supported by the similar lack of such images from previous works (Bouharmont 1960; Cope 1940, 1962). Subsequent intracellular movement of the sperm nucleus to the egg nucleus was predominantly complete by 36 h after pollination (Table 1) and so occurred within 12–28 h of entry into the embryo sac. As in cotton, the closest model relative of cocoa, sperm cells travel the circumference of the egg prior to alignment with the egg nucleus (Jensen

Table 1 Progression of sperm nuclei towards the egg nucleus and nearest polar nucleus following compatible and incompatible pollination

	Sperm nucleus to egg nucleus		Sperm nucleus to polar nucleus	
	Compatible ovules	Incompatible ovules	Compatible ovules	Incompatible ovules
24 h After pollination	1.63	a	6.59	a
	3.06	6.29	17.02	10.33
	5.20	10.10	25.15	23.96
	4.08	7.68	12.62	22.80
	8.79	8.56	17.24	17.21
	5.04	a	20.48	0.60
	16.93	3.11	20.21	13.67
	7.02	4.25	10.38	14.48
	a	1.02	0.72	12.11
	15.51	20.53	22.02	20.94
Mean	7.47	7.69	15.24	15.12
Standard deviation	5.39	5.98	7.60	7.25
Standard error	1.79	2.11	2.4	2.41
t test	$p = 0.938$, NS		$p = 0.972$, NS	
36 h After pollination	f	5.56	1.32	10.67
	f	1.85	f	7.27
	f	a	f	3.22
	f	1.92	f	10.61
	1.05	a	3.06	a
	f	2.94	f	3.53
	3.86	a	19.08	a
	7.21	3.86	24.78	11.36
	f	3.62	f	16.98
	f	2.83	f	15.29
Mean	4.04	3.23	12.06	9.87
Standard deviation	3.08	1.28	11.65	4.99
Standard error	1.78	0.48	5.83	1.77
t test	$p = 0.552$, NS		$p = 0.649$, NS	
48 h After pollination	f	a	f	2.99
	f	1.52	f	2.08
	f	a	f	2.31
	f	a	f	a
	f	a	f	a
	f	11.52	f	11.62
	f	7.20	f	11.68
	f	2.80	f	11.98
	f	6.11	f	19.89
	f	a	f	2.39
	f	1.83	f	7.65
	f	a	f	a
	f	a	f	a
	f	0.56	f	1.13
	f	a	f	a
	f	a	f	a
Mean	–	4.51	–	7.37
Standard deviation	–	3.66	–	5.93
Standard error		1.49		1.97
t test	–		–	

Measurements on the same row of the table are from the same compatible/incompatible ovule. Remaining separation distance in μm; *a* adjacent/in contact, *f* fused

1965; Jensen and Fisher 1968) with nuclear fusion occurring on the side of the egg nucleus furthest from the point of sperm entry into the egg cell. Measurements of the unfertilised egg cell and newly formed zygote revealed that the fusion of egg and sperm nuclei resulted in only a modest increase in mean volume (occurring between 24 and 36 h post-pollination). This slight expansion was followed by a substantive increase in nuclear volume by 48 h after pollination: perhaps, the most plausible explanation for the increase being the de novo synthesis of DNA during post-fusion nuclear S-phase.

The second sperm nucleus reaches the polar nuclei only slightly later (Fig. 3b, d), again with fusion occurring in the majority of ovules within 12–36 h of entry into the embryo sac (Table 1). The high level of resolution afforded by confocal microscopy allowed detailed observations on post-fertilisation development of the polar nuclei. Sperm cell delivery to the central cell still occurs some 24 h after pollination, at which point the latter contains two polar nuclei, each possessing a single nucleolus (Fig. 3d). This is concurrent with the observations of Bouharmont (1960), who reported that the formation of a single diploid, primary endosperm nucleus from the fusion of the two polar nuclei does not take place prior to sperm release in cocoa. At 36 h after pollination, sperm nuclei can no longer be seen within the embryo sac and karyogamy is therefore assumed to have taken place (Fig. 4a, b), although the central cell still contains two distinct nuclei (Fig. 4a). Bouharmont (1960) similarly reported the presence of two nuclei at this stage, but we were also able to show that their volumes differ significantly in size. We infer that the larger of these two nuclei is the diploid product of the fusion between the sperm nucleus and one polar nucleus and that the second, smaller nucleus is the remaining haploid polar nucleus. This pattern matches the classic work of Navashin (1898) in which angiosperm 'double fertilisation' was first described in *Fritillaria* and *Lilium*. However, unlike these and other exemplars, subsequent nuclear fusions leading to creation of a triploid primary endosperm nucleus were not evident in cocoa during this period. At 96 h after pollination, there were still two nuclei within the central cell; thus, there is no evidence of the further development of a primary endosperm nucleus within this time period (Fig. 4; Supplementary Data, Figs. S1-S2). Indeed, Bouharmont (1960) described a protracted development of the primary endosperm nucleus continuing over a number of days, suggesting that the time course of the current study was insufficient to capture its formation.

In broad terms, our images of sperm nucleus progression towards the egg nucleus confirm previous observations of gametic 'non-fusion' following incompatible pollination (Bennett and Cope 1959; Bouharmont 1960; Cope 1958, 1962). However, despite the relatively low numbers of ovules observed, the number of fusion ovules following incompatible pollination in SCA 24 (9/107) does not readily fall into any of the categories defined by Cope (1958, 1962). The increased resolution and enhanced ability to measure intracellular distances provided by confocal microscopy allowed differentiation between instances where gametic nuclear fusion had failed and those cases where sperm nucleus migration was incomplete.

These observations have also revealed some instances where the sperm-egg nuclear fusion/delivery was complete, but sperm-polar nucleus was not. This was observed for two compatibly pollinated ovules at 24 and 36 h after pollination (sperm-egg nuclei adjacent, sperm-polar nuclei 0.72 μm apart; sperm-egg nuclear fusion complete, sperm-polar nuclei 1.32 μm apart, respectively) and five incompatibly pollinated ovules at 24 h (sperm-egg nuclei adjacent, sperm-polar nuclei 0.60 μm apart), 36 h (sperm-egg nuclei adjacent, sperm-polar nuclei 3.22 μm apart) and three at 48 h (sperm-egg nuclei adjacent, sperm-polar nuclei 2.31–2.99 μm apart) (Table 1). If sperm-egg nuclear fusion occurs prior to sperm-polar nuclear fusion, then the occurrence of a differential should perhaps be expected in some ovules. At 36 h after pollination, the remnant sperm nucleus in the incompatible ovule is nearly 2.5 × further away from the polar nucleus than in the compatible ovule at the same time. The incompatible remnant sperm nuclei are only marginally closer to the polar nucleus at 48 h than at 36 h after pollination. A differential delivery reaction between sperm and egg and sperm and polar nuclei within the same ovule is unlikely to be genetic in nature as both female and male gametes in each case would be carrying the same compatibility alleles. We speculate that these data may therefore be indicative of a slowing of the motor processes that transport the sperm nuclei towards their target nuclei, which would be more apparent for sperm nuclei migrating towards the central cell due to the greater distance of travel.

The self-incompatibility reaction of *T. cacao* is known to be complex and spans 100 % compatibility, partial compatibility, through to 100 % incompatibility, the reaction itself involving several processes (gametic nuclear fusion/non-fusion, peduncle thickening/floral abscission). It is possible that delayed migration of self-gamete nuclei is rare or even unique to SCA 24 and may not have been previously recorded because it has not been seen. To our knowledge, this is the first cytological examination of SI in SCA 24. Knight and Rogers (1953, 1955) and Cope (1962) worked on similar material derived from crosses between NA 32, PA 7 [POU] and PA 35 [POU]. Cope (1962) also worked extensively on ICS material but included SCA 6 and SCA 12 in some experiments. These two clones originate from the same expedition to the River Ucayali in Peru as SCA 24 (Turnbull and Hadley 2011) and both were

shown to be self- and cross-incompatible, with SCA 6 displaying 50 % 'non-fusion' ovules following self-pollination (Cope 1962). Thus, the complete range of the incompatibility response in cocoa may not be entirely known, and the broader importance of delayed migration requires further study before generalisations can be made.

If the operation of delayed sperm nucleus delivery does occur more frequently throughout the species, the absence of karyogamy is no longer simply a function of the proportion of non-fusion events, but also requires consideration of gamete nucleus delivery. Intriguingly in SCA 24, incompatible ovules can be divided between instances of 'non-fusion' and incomplete delivery in a 1:1 ratio (Table 1). This is suggestive of a gametophytic control of sperm nucleus delivery. One possible explanation is that SCA 24 possesses both functional and non-functional alleles of a gene responsible for sperm nucleus migration to the maternal gametic nuclei. The fact that only some of the delivered sperm nuclei fused with their maternal target nuclei suggests that the 'non-fusion' of gamete nuclei may be an independent process to 'incomplete nucleus delivery' and that the two systems may act in an additive manner.

Cope (1962) noted that the most commonly observed segregation pattern among ovules of SI cocoa clones following self-pollination was 1:3 'non-fused':'fused' ovules. He also noted that this segregation pattern is consistent with gametophytic control if there are two independent haploid constituents acting to cause non-fusion. The suggestion here is that gamete nucleus migration and nuclear fusion operate independently and conform to segregation ratios expected from gametophytic control in SCA 24. If confirmed, this explanation may therefore provide an enticing new avenue with which to investigate the wider phenomenon of LSI in cocoa. The present study does not have sufficient data to draw such firm conclusions, however, and a larger and much broader cytological examination of LSI is required to address this issue.

Further detailed cytological observations of double fertilisation may also assist molecular efforts that seek to gain a mechanistic understanding of the LSI process in cocoa. Recent real-time investigations into the mechanism propelling the sperm cell towards the egg cell in *Arabidopsis* suggest that cytoplasmic flow following pollen tube rupture rapidly (<1 min) carries the released sperm cells to the female gamete plasma membranes (Hamamura et al. 2011). Once positioned between the egg cell and central cell, sperm cells pause briefly (approx. 7 min) prior to membrane fusion and subsequent release of male gamete nuclei into the egg cell/central cell (Hamamura et al. 2011). Gametic membrane fusion (plasmogamy) involves male–female gamete recognition and male gamete-specific genes acting on the plasma membrane (Faure et al. 1994; Xu et al. 1999). The sperm-specific *HAP2/GCS1* gene is requisite for fusion (Mori et al. 2006; von Besser et al. 2006) and encodes a highly conserved membrane protein that may be a molecular trigger for gamete fusion. The pause observed at the point of membrane contact prior to plasmogamy may thus serve to allow intercellular communication between the two sperm cells and/or the egg cell and central cell via these genes (Hamamura et al. 2011). This interaction between gametic membranes offers a potential opportunity for self-allele recognition and thus rejection. Clearly, complete failure of gametic membrane fusion would preclude entry of the sperm nuclei into the egg cell/central cell and so cannot be the underlying system observed in SCA 24. It is nevertheless possible that self-recognition leads to delayed, rather than failed, plasmogamy and so ultimately leads to slowed delivery of male gametic nuclei as observed in this clone. A more direct explanation of slowed progression of the male nucleus within the egg cell/central cell is also possible. Following plasmogamy, sperm nuclei actively migrate towards the female nuclei (Berger 2011), possibly via the formation of actin filaments as observed in tobacco and *Torenia* (Fu et al. 2000; Huang and Russell 1994). Recently developed markers for actin microtubules (Era et al. 2009; Oh et al. 2010) should allow this to be determined using live-imaging confocal microscopy (Berger 2011), but further work is still required to identify the genes involved in this process. It is also plausible that any delay in migration could result in the loss of phase synchrony between male and female nuclei, resulting in an inability to effect fusion (Friedman 1999).

The use of live-cell imaging confocal microscopy has led to a recent increase in our knowledge of the processes involved in double fertilisation (Hamamura et al. 2011) and offers the potential to unlock many of the remaining elusive mechanisms in operation (Berger 2011). Future developments in this area may also assist in the investigation of post-pollination events in the many species displaying LSI and unlock the enigmatic system of self-rejection in cocoa. Our findings suggest that future studies aiming to derive a genetic understanding of the LSI process in cocoa should (as here) distinguish between the two cytological events of nuclear migration and fusion. In the nearer future, further studies in *Theobroma grandiflorum*, where delayed sperm delivery is evident but where 'non-fusion' is not (Ramos et al. 2005), may provide additional insights into the evolution of self-incompatibility within this and related species.

Acknowledgments This work was funded by the Biscuit, Cake, Chocolate and Confectionary Alliance (now Cocoa Research Association) of the UK and was conducted at the Department of Biological Sciences, University of Reading, UK. Many thanks to Professor Paul Hadley and Mr. Stephen Poutney.

References

Allen AM, Hiscock SJ (2008) Evolution and phylogeny of self-incompatibility systems in angiosperms. In: Franklin-Tong VE (ed) Self-incompatibility in flowering plants—evolution, diversity and mechanisms. Springer, Berlin, pp 73–101

Alverson WS, Karol KG, Baum DA, Chase MW, Swensen SM, McCourt R, Sytsma KJ (1998) Circumscription of the Malvales and relationships to the other Rosidae: evidence from *rbcL* sequence data. Am J Bot 85:876–887

Aneja M, Gianfagna T, Ng E (1999) The roles of abscisic acid and ethylene in the abscission and senescence of cocoa flowers. Plant Growth Regul 27:149–155

Baker RP, Hasenstein KH, Zavada MS (1997) Hormonal changes after compatible and incompatible pollination in *Theobroma cacao* L. HortSci 32:1231–1234

Beardsell DV, Knox RB, Williams EG (1993) Breeding system and reproductive success of *Thryptomene calycina* (Myrtaceae). Aust J Bot 41:333–353

Bennett MC, Cope FW (1959) Nuclear fusion and non-fusion in *Theobroma cacao* L. Nature 183:1540

Berger F (2011) Imaging fertilization in flowering plants, not so abominable after all. J Exp Bot 62:1651–1658

Bouharmont J (1960) Recherches cytologiques sur la fructification et l'incompatibilité chez *Theobroma cacao* L. Publication de l'Institut National pour l'Étude Agronomique du Congo, Série Scientifique No. 89

Braselton JP, Wilkinson MJ, Clulow SA (1996) Feulgen staining of intact plant tissues for confocal microscopy. Biotech Histochem 71:84–87

Cheesman EE (1927) Fertilisation and embryogeny in *Theobroma cacao,* L. Ann Bot 41:107–126

Cheesman EE (1932) The economic botany of cacao: a critical survey of the literature to the end of 1930. Trop Agric S9:1–16

Cope FW (1939) Studies in the mechanism of self-incompatibility in cacao I. Eighth Annual Report on Cocoa Research, Trinidad, pp 20–21

Cope FW (1940) Studies in the mechanism of self-incompatibility in cacao II. Ninth Annual Report of Cocoa Research, Trinidad, pp 19–23

Cope FW (1958) Incompatibility in *Theobroma cacao*. Nature 181:279

Cope FW (1962) The mechanism of pollen incompatibility in *Theobroma cacao* L. Heredity 17:157–182

de Sousa MS, Venturieri GA (2010) Floral biology of cacauhy (*Theobroma speciosum*—Malvaceae). Braz Arch Biol Technol 53:861–872

Efombagn MIB, Sounigo O, Eskes AB, Motamajor JC, Manzanares-Dauleux MJ, Schnell R (2009) Parentage analysis and outcrossing patterns in cacao (*Theobroma cacao* L.) farms in Cameroon. Heredity 103:46–53

Era A, Tominaga M, Ebine K, Awai C, Saito C, Ishizaki K, Yamato KT, Kohchi T, Nakano A, Ueda T (2009) Application of Lifeact reveals F-actin dynamics in *Arabidopsis thaliana* and the liverwort, *Marchantia polymorpha*. Plant Cell Physiol 50:1041–1048

Faure J-E, Digonnet C, Dumas C (1994) An in vitro fusion system of adhesion and fusion in maize gametes. Science 263:1598–1600

Friedman WE (1999) Expression of the cell cycle in sperm of *Arabidopsis:* implications for understanding patterns of gametogenesis and fertilization in plants and other eukaryotes. Development 126:1065–1075

Fu Y, Yuan M, Huang BQ, Yang HY, Zee SY, Tp OB (2000) Changes in actin organization in the living egg apparatus of *Torenia fournieri* during fertilization. Sex Plant Reprod 12:315–322

Gibbs PE, Bianchi M (1993) Post-pollination events in species of *Chorisia* (Bombacaceae) and *Tabebuia* (Bignoniaceae) with late-acting self-incompatibility. Bot Acta 106:64–71

Gibbs PE, Bianchi M (1999) Does late-acting self-incompatibility (LSI) show family clustering? Two more species of Bignoniaceae with LSI: *Dolichandra cynanchoides* and *Tabebuia nodosa*. Ann Bot 84:449–457

Gigord L, Lavigne C, Shykoff JA (1998) Partial self-incompatibility and inbreeding depression in a native tree species of La Réunion (Indian Ocean). Oecologia 117:342–352

Gribel R, Gibbs PE (2002) High outbreeding as a consequence of selfed ovule mortality and single vector bat pollination in the Amazonian tree *Pseudobombax munguba* (Bombacaceae). Int J Plant Sci 163:1035–1043

Gribel R, Gibbs PE, Queiros AL (1999) Flowering phenology and pollination biology of *Ceiba pentandra* (Bombacaceae) in Central Amazonia. J Trop Ecol 15:247–263

Hamamura Y, Saito C, Awai C, Kurihara D, Miyawaki A, Nakagawa T, Kanaoka MM, Sasaki N, Nakano A, Berger F, Higashiyama T (2011) Live-cell imaging reveals the dynamics of two sperm cells during double fertilization in *Arabidopsis thaliana*. Curr Biol 21:497–502

Hasenstein KH, Zavada MS (2001) Auxin modification of the incompatibility response in *Theobroma cacao*. Physiol Plant 112:113–118

Huang BQ, Russell SD (1994) Fertilisation in *Nicotiana tabacum*: cytoskeletal modification in the embryo sac during synergid degradation. A hypothesis for short-distance transport of sperm cells prior to gamete fusion. Planta 194:200–214

Jacob VJ (1973) Self-incompatibility mechanism in *Cola nitida*. Incompat Newsl 3:60–61

Jensen WA (1965) The ultrastructure and histochemistry of the synergids of cotton. Am J Bot 52:238–256

Jensen WA, Fisher DB (1968) Cotton embryogenesis: the entrance and discharge of the pollen tube in the embryo sac. Planta 78:158–183

Kawagoe T, Suzuki N (2005) Self-pollen on a stigma interferes with outcrosses seed production in a self-incompatible monoecious plant, *Akebia quinata* (Lardizabalaceae). Funct Ecol 19:49–54

Knight R, Rogers HH (1953) Sterility in *Theobroma cacao* L. Nature 172:164

Knight R, Rogers HH (1955) Incompatibility in *Theobroma cacao*. Heredity 9:69–77

Knox RB, Williams EB, Dumas C (1986) Pollen, pistil and reproductive function in crops plants. Plant Breed Rev 4:9–73

LaDoux T, Friar EA (2006) Late-acting self-incompatibility in *Ipomopsis tenuifolia* (Gray) V. Grant (Polemoniaceae). Int J Plant Sci 167:463–471

Lanaud C, Sounigo O, Amefia YK, Paulin D, Lachenaud P, Clément D (1987) Nouvelles données sur le fontionnement du système d'incompatibilité du cacaoyer et ses consequences pour la selection. Café Cacao Thé 31:267–277

Lockwood G (1979) Cocoa breeding in Ghana with reference to swollen shoot disease. 7th International Cocoa Research Conference, Douala, Cameroon, pp 407–413

McKay JW (1942) Self-sterility in the chinese chestnut (*Castanea mollissima*). Proc Am Soc Hort Sci 41:156–160

Mori T, Kuroiwa H, Higashiyama T, Kuroiwa T (2006) Generative cell specific 1 is essential for angiosperm fertilization. Nat Cell Biol 8:64–71

Navashin SG (1898) Resultate einer Revision der Befruchtungsvorgange bei *Lilium martagon* und *Fritillaria tenella*. Bull Acad Sci St. Petersburg 9:377–382

Oh SA, Pal MD, Park SK, Johnson JA, Twell D (2010) The tobacco MAP215/Dis1 family protein TMB200 is required for the

functional organisation of microtubule arrays during male germline establishment. J Exp Bot 61:969–981
Oliveira PE, Gibbs PE (2000) Reproductive biology of woody plants in a cerrado community of Central Brazil. Flora 195:311–329
Pound FJ (1932) Studies of fruitfulness in cacao II. Evidence for partial self-sterility. First Annual Report on Cocoa Research, Trinidad, pp 24–28
Ramos AR, Venturieri GA, Cuco SM, Castro NM (2005) The site of self-incompatibility in cupuassu (*Theobroma grandiflorum*). Rev Bras Bot 28:569–578
Reyes EH (1979) Mejoramiento genetic del cacao en Venezuela. 7th International cocoa research conference, Douala, Cameroon, pp 513–518
Sage TL, Sampson FB (2003) Evidence for ovarian self-incompatibility as a cause of self-sterility in the relictual woody angiosperm *Pseudowintera axillaris* (Winteraceae). Ann Bot 91:807–816
Sage TL, Williams EG (1991) Self-incompatibility in Asclepias. Plant Cell Incomp Newsl 23:55–57
Sage TL, Bertin TI, Williams EG (1994) Ovarian and other late-acting self-incompatibility systems. In: Williams EG, Clark AE, Knox RB (eds) Genetic control of self-incompatibility and reproductive development in flowering plants. Kluwer Academic Publishing, Dordrecht, pp 116–140
Sage TL, Strumas F, Cole WW, Barrett SCH (1999) Differential ovule development following self- and cross-pollination: the basis of self-sterility in *Narcissus triandrus* (Amaryllidaceae). Am J Bot 86:855–870
Sauer JD (1994) Historical geography of crop plants: a select roster. CRC Press, Boca Raton
Seavey SR, Bawa KS (1986) Late-acting self-incompatibility in angiosperms. Bot Rev 52:195–219
Soria VJ (1978) The breeding of cacao (*Theobroma cacao* L.). Trop Agric Res Ser 11:161–168
Taroda N, Gibbs PE (1982) Floral biology and breeding system of *Sterculia chicha* St. Hil (Sterculiaceae). New Phytol 90:342–743
Turnbull CJ, Hadley P (2011) International cocoa germplasm database (ICGD) online database. http://www.icgd.reading.ac.uk. Accessed 15th July 2011
Vaughton G, Ramsey M, Johnson SD (2010) Pollination and late-acting self-incompatibility in *Cyrtanthus breviflorus* (Amaryllidaceae): implications for seed production. Ann Bot 106:547–555
von Besser K, Frank AC, Johnson MA, Preuss D (2006) *Arabidopsis* HAP2 (GCS1) is a sperm specific gene required for pollen tube guidance and fertilization. Development 133:4761–4769
Williams EG, Kaul V, Rouse JL, Knox RB (1984) Apparent self-incompatibility in *Rhododendron ellipticum, R. championae* and *R. amamiense*: a post-zygotic mechanism. Plant Cell Incomp Newsl 16:10–11
Xu H, Swoboda I, Bhalla PL, Singh MB (1999) Male gametic cell-specific gene expression in flowering plants. Proc Nat Acad Sci USA 96:2554–2558